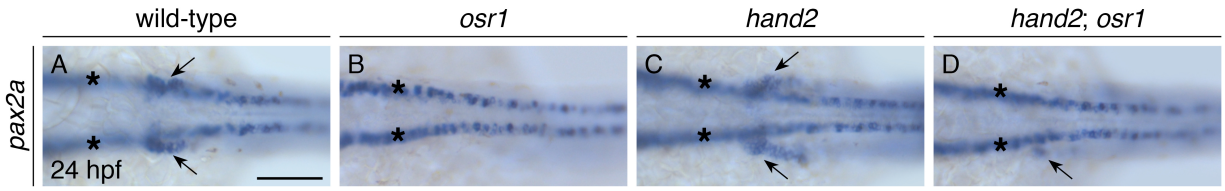

Figure S1. Proximal pronephron defects in *osr1* mutants are partially suppressed by *hand2* loss-of-function.

(A-D) Dorsal views, anterior to the left, of wild-type (A), *osr1* mutant (B), *hand2* mutant (C), and *hand2*; *osr1* double mutant (D) embryos at 26 hpf. In situ hybridization shows *pax2a* expression in the glomerular precursors and the neck region (arrows) of the pronephron. Compared to wild-type (A), *pax2a* expression is absent in *osr1* mutants (B), expanded in *hand2* mutants (C), and most similar to wild-type in *hand2*; *osr1* double mutants (D). Expression in overlying spinal neurons (asterisks) is unaffected.

Scale bar: 25 μm.

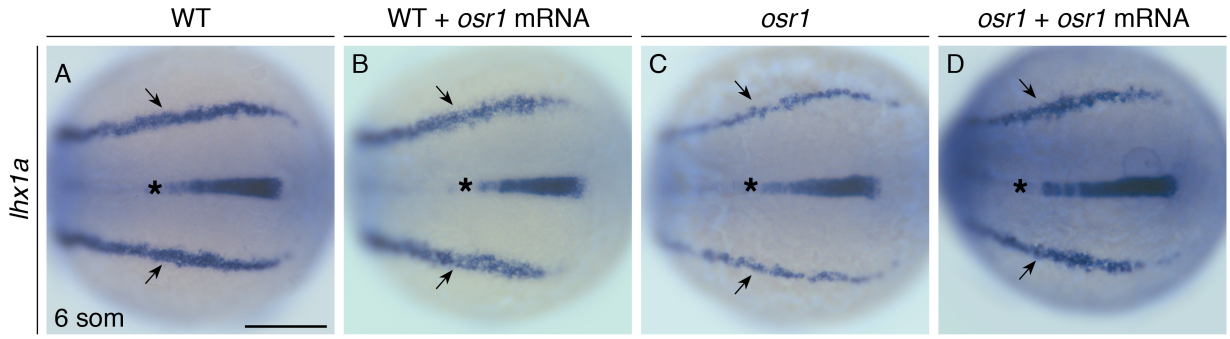

Figure S2. *osr1* mRNA injection rescues intermediate mesoderm defects in *osr1* mutants.

(A-D) Dorsal views, anterior to the left, of wild-type (A,B) and *osr1* mutant (C,D) embryos at 6 som. In situ hybridization shows expression of *lhx1a* in the IM (arrows). Compared to wild-type (A), *lhx1a* expression is narrowed in *osr1* mutant embryos (C). Following injection with wild-type *osr1* mRNA at the one-cell stage, *lhx1a* expression in *osr1* mutant embryos (D) appears comparable to that seen in wild-type embryos (A) or injected wild-type embryos (B). 85% of 27 uninjected *osr1* mutants exhibited narrowed expression in the IM, whereas only 4% of 80 uninjected wild-type siblings exhibited similarly narrowed expression ($P<0.0001$, Fisher's exact test). In contrast, following injection with wild-type *osr1* mRNA, only 31% of 16 *osr1* mutants exhibited similarly narrowed expression in the IM, and only 2% of 55 wild-type siblings exhibited narrowed expression. These data indicate a statistically significant rescue of the IM defects in *osr1* mutant embryos following injection with wild-type *osr1* mRNA ($P=0.00007$, Fisher's exact test). Expression of *lhx1a* in the notochord (asterisk) is unaffected. Scale bar: 100 μm.

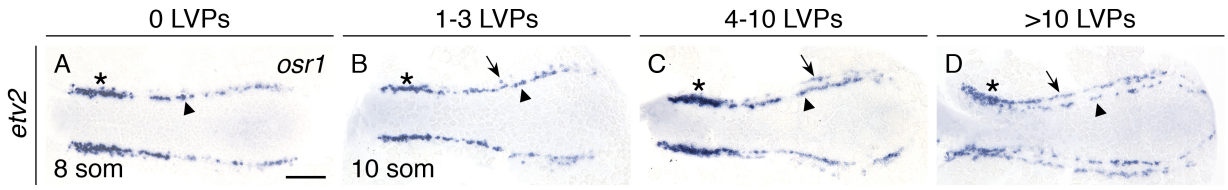

E

Age	Genotype	Presence of LVPs			Number of LVPs		
		Absent	Present	Fisher's exact test	1-3	4-10	> 10
6 som	wild-type	100% (54/54)	0% (0/54)	0.0024	0% (0/54)	0% (0/54)	0% (0/54)
	osr1	80% (20/25)	20% (5/25)		12% (3/25)	8% (2/25)	0% (0/25)
8 som	wild-type	85% (60/71)	15% (11/71)	0.0001	11% (8/71)	4% (3/71)	0% (0/71)
	osr1	24% (5/21)	76% (16/21)		24% (5/21)	43% (9/21)	9% (2/21)
10 som	wild-type	45% (34/75)	55% (41/75)	0.0001	47% (35/75)	8% (6/75)	0% (0/75)
	osr1	0% (0/25)	100% (25/25)		16% (4/25)	24% (6/25)	60% (15/25)
13 som	wild-type	0% (0/60)	100% (60/60)	1.0000	0% (0/60)	0% (0/60)	100% (60/60)
	osr1	0% (0/22)	100% (22/22)		0% (0/22)	0% (0/22)	100% (22/22)

Figure S3. Premature lateral vessel progenitors in *osr1* mutant embryos.

(A-D) Dorsal views, anterior to the left, of *osr1* mutant embryos at 8 som (A) and 10 som (B-D). In situ hybridization demonstrates that *etv2* is expressed bilaterally in medial (arrowheads) and lateral (arrows) territories. Representative examples are shown for embryos with 0 LVPs (A), 1-3 LVPs (B), 4-10 LVPs (C), and >10 LVPs (D). Embryos were categorized based on the number of cells observed on whichever side of the mesoderm exhibited more LVPs. Note the increased *etv2* expression in the most proximal portion of the posterior mesoderm (asterisks), a phenotype also seen with *flk1* expression (Fig. S5); this phenotype was observed previously in *osr1* morphants (Mudumana et al., 2008).

(E) Percentages of embryos and corresponding fractions in each category, as summarized in Fig. 3E. At each stage, the proportions of embryos with and without LVPs were compared between *osr1* mutants and their wild-type siblings using Fisher's exact test; *P* values are provided for each comparison. At 8 som and 10 som, and to a lesser degree at 6 som, we observed significantly more *osr1* mutant embryos with LVPs than wild-type siblings with LVPs.

Scale bar: 100 μm.

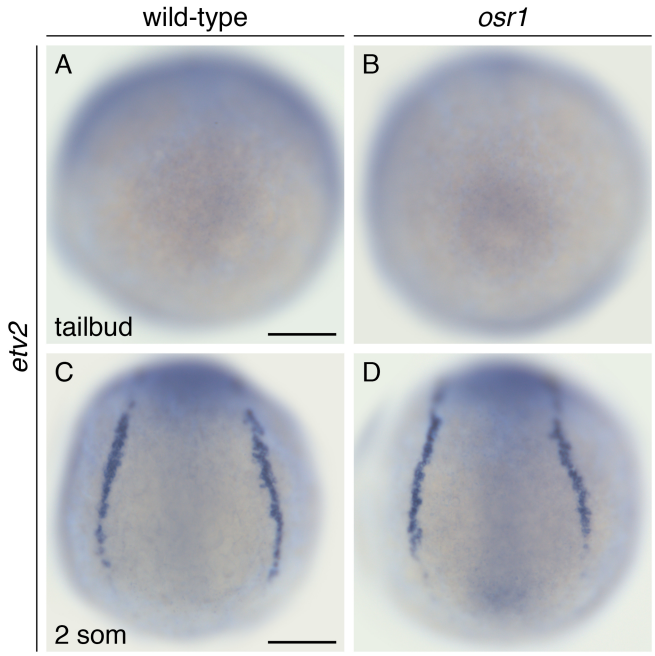

Figure S4. Medial vessel progenitors appear unaffected in *osr1* mutant embryos. (A-D) Dorsal views, anterior to the top, of wild-type (A,C) and *osr1* mutant (B,D) embryos at tailbud (A,B) and 2 som (C,D). Previous studies have shown that the medial vessel progenitors express *etv2* beginning at 2 som (Reischauer et al., 2016). In situ hybridization demonstrates that *etv2* is not expressed in either wild-type (A, n=69) or *osr1* mutant (B, n=21) embryos at tailbud stage. At 2 som, *etv2* expression is evident in wild-type (C, n=33) and appears comparable in *osr1* mutant (D, n=8) embryos.
Scale bar: 100 μm.

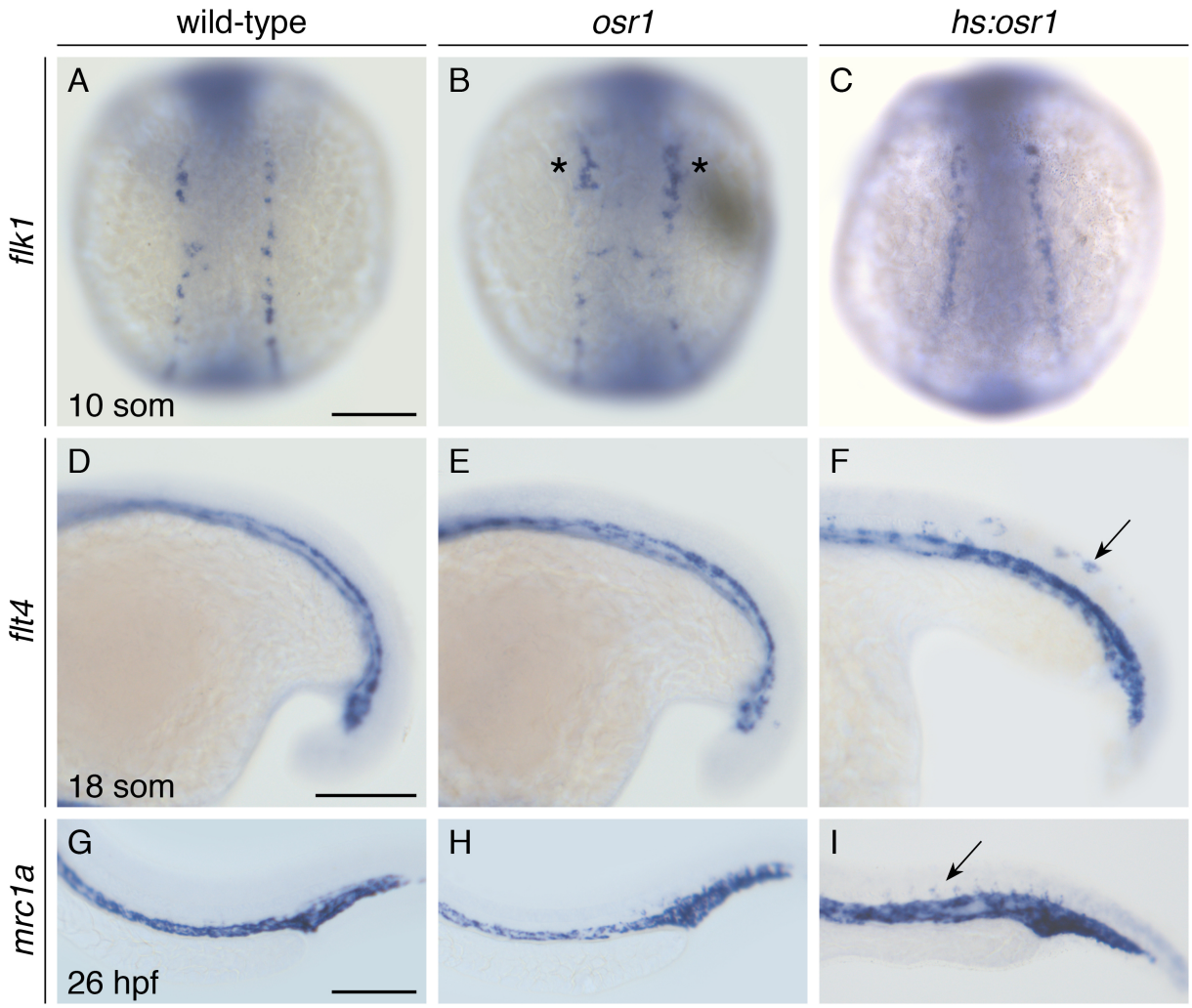

Figure S5. Effects of *osr1* loss-of-function and gain-of-function on vessel progenitors and vasculature.

In situ hybridization shows *flk1* expression at 10 som **(A-C)**, *flt4* expression at 18 som **(D-F)**, and *mrc1a* expression at 26 hpf **(G-I)** in dorsal views, anterior to the top (A-C), or lateral views, anterior to the left (D-I), of wild-type (A,D,G), *osr1* mutant (B,E,H), and *Tg*(*hsp70:osr1-t2A-BFP*) (*hs:osr1*) (C,F,I) embryos. (A,B) Like *etv2* (Fig. 3, Fig. S3), and similar to prior studies of *osr1* morphants (Mudumana et al., 2008), *flk1* expression is increased proximally in *osr1* mutants (B, asterisks); this phenotype was observed in 82% of *osr1* mutants (n=17) and in 0% of wild-type embryos (n=43). (C) Like *etv2* expression in the medial vessel progenitors (Fig. 4, Fig. S7), *flk1* expression was mildly increased by *osr1* overexpression (20% of *hs:osr1* embryos, n=56). (D-I) Previously, we observed defects in *flt4* and *mrc1a* expression in the cardinal vein and dorsal aorta of embryos with altered *hand2* function (Perens et al., 2016). Specifically, expression of both genes was absent in the cardinal vein of *hand2* mutants, and expression of both genes appeared increased by *hand2* overexpression. We assessed whether expression of these genes was altered in the cardinal vein and dorsal aorta of *osr1* mutant and *hs:osr1* embryos. Expression of both *flt4* and *mrc1a* appeared comparable in wild-type (D,G) and *osr1* mutant (E,H) embryos within the cardinal vein and dorsal aorta (*flt4*: wild-type, n=52; *osr1*, n=14; *mrc1a*: wild-type, n=31; *osr1*, n=12), but expression of both genes was increased in all *hs:osr1* embryos (F,I), including areas of ectopic expression (arrows) within the trunk (ectopic *flt4* in 59% of *hs:osr1* embryos, n=52; ectopic *mrc1a* in 14% of *hs:osr1* embryos, n=22).

Scale bars: 100 μm.

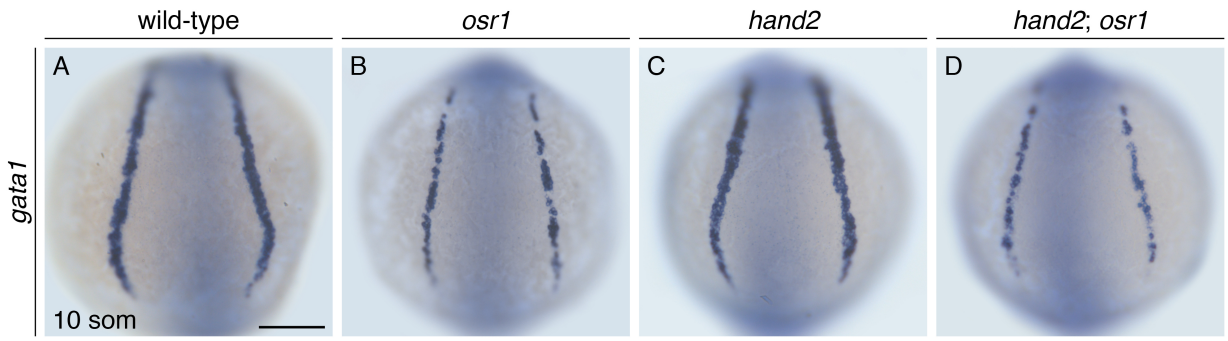

Figure S6. *hand2* loss-of-function does not suppress the blood progenitor defects in *osr1* mutants.

(A-D) Dorsal views, anterior to the top, of wild-type (A), *osr1* mutant (B), *hand2* mutant (C), and *hand2*; *osr1* double mutant embryos (D*)* at 10 som. In situ hybridization shows *gata1* expression in blood progenitors. Compared to wild-type (A), *gata1* expression is decreased throughout the posterior mesoderm in *osr1* mutants (B), unchanged in *hand2* mutants (C), and relatively similar to *osr1* mutants in *hand2*; *osr1* double mutant embryos (D). In contrast, *osr1* morphants were shown to exhibit reduction in *gata1* expression only at the proximal end of the *gata1* expression domain (Mudumana et al., 2008).

Scale bar: 100 μm.

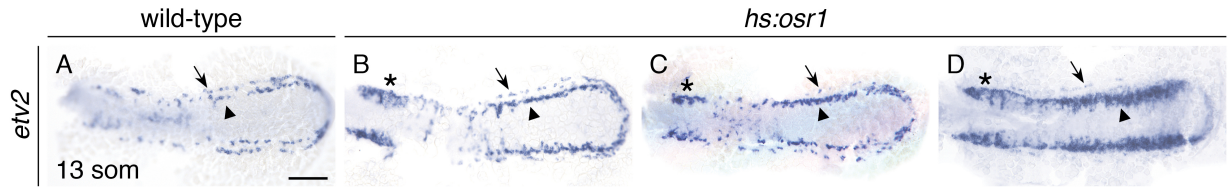

Figure S7. Overexpression of *osr1* yields a range of vessel progenitor phenotypes. (A-D) Dorsal views, anterior to the left, of wild-type (A) and *hs:osr1* embryos (B-D) at 13 som. (A) In situ hybridization demonstrates that *etv2* is expressed in medial (arrowheads), lateral (arrows), and proximal (asterisk) territories within the wild-type posterior mesoderm. (B-D) In *hs:osr1* embryos (n=58), a range of phenotypes was observed, including mildly increased medial expression with mildly reduced lateral expression (B, 40% of embryos), moderately increased medial expression with greatly reduced lateral expression (C, 36% of embryos), and greatly expanded territory of medial expression with absent lateral expression (D, 24% of embryos). We could not distinguish whether the suppression of LVP formation was due to a delay of LVP formation or a complete inability to form LVPs; after 14 som, the vessel progenitors migrate toward the midline and the medial and lateral vessel progenitors become indistinguishable, as there are no known molecular markers that distinguish the two populations (Kohli et al., 2013). Surprisingly, the proximal *etv2* expression territory appeared expanded in *hs:osr1* embryos (B-D, asterisks), similar to the *osr1* mutant phenotype (Fig. 3D,G). Taken together, the divergent responses of each of the *etv2*-expressing territories to *osr1* loss-of-function and gain-of-function suggest that *osr1* plays a different, and possibly independent, role in the regulation of each vessel progenitor territory. It is intriguing to consider whether these differences in regulation correlate with the subpopulations of *etv2*-expressing cells distinguished by unique transcriptional signatures, as determined by single-cell RNA-sequencing (Chestnut et al., 2020).
Scale bar: 100 μm.

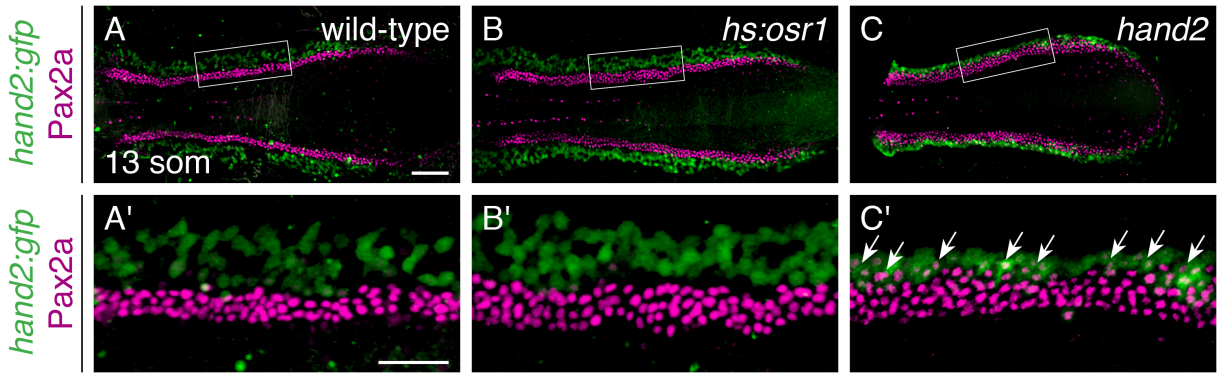

Figure S8. Unlike in *hand2* mutants, increased Pax2a in *hs:osr1* embryos is not observed in *hand2*-expressing cells.

(A-C) Three-dimensional reconstructions of Pax2a and GFP immunofluorescence in wild-type (A), *hs:osr1* (B), and *hand2* mutant (C) embryos carrying *Tg(hand2:egfp)*; dorsal views, anterior to the left, at 13 som. (A',B') Magnification of boxed 250 μm long regions. Compared to wild-type (A) and *hs:osr1* (B) embryos, *hand2* mutant embryos (C) have a noticeable increase in the presence of Pax2a in *hand2*-expressing cells (arrows). Stronger *hand2:egfp* expression in *hand2* mutants is consistent with our prior results (Perens et al., 2016).

Scale bars: 100 μm (A-C), 50 μm (A'-C').

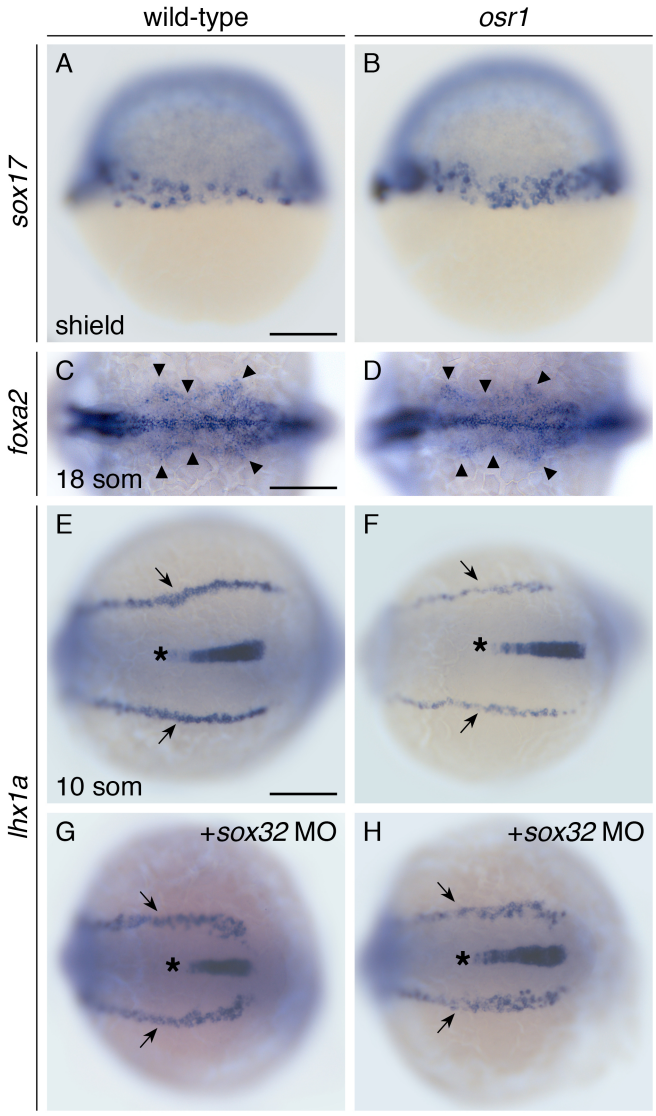

Figure S9. Examination of endoderm formation and the effects of *sox32* knockdown in *osr1* mutant embryos.

(A-D) Lateral views, dorsal to the left, at shield stage (A,B); dorsal views, anterior to the left, at 18 som (C,D), in wild-type (A,C) and *osr1* mutant (B,D) embryos. In situ hybridization shows *sox17* expression in endoderm progenitors (A,B) and *foxa2* expression in the pharyngeal endoderm (arrowheads) (C,D). At shield stage, we observed a trend toward an increased amount of *sox17*-expressing endoderm progenitors at the blastoderm margin of *osr1* mutants. Specifically, 86% of 22 *osr1* mutant embryos appeared to have an excess of *sox17*-expressing endoderm progenitors, whereas only 14% of 81 wild-type siblings had a similar appearance ($P<0.0001$, Fisher's exact test). Similarly, *osr1* morphants were reported to have an increased number of tiers of *sox17*-expressing cells, compared to that seen in wild-type embryos (Mudumana et al., 2008). (C,D) However, although endodermal expression of *foxa2* was reported to be increased in *osr1* morphants at 18 som (Mudumana et al., 2008), we did not observe any consistent difference in the *foxa2*-expressing endoderm when comparing wild-type (n=61) and *osr1* mutant (n=19) embryos.

(E-H) Dorsal views, anterior to the left, at 10 som in wild-type (E,G), and *osr1* mutant (F,H) embryos. In situ hybridization shows *lhx1a* expression in the IM (arrows). In prior studies, disruption of endoderm formation via *sox32* knockdown appeared to partially rescue the pronephron tubule defects in *osr1* morphants (Mudumana et al., 2008; Tomar et al., 2014). We found that injection of a *sox32* morpholino (MO) broadened the morphology of the IM in both wild-type (G, n=24) and *osr1* mutant (H, n=14) embryos, compared to the IM of uninjected siblings (E,F). Similarly, multiple mesodermal derivatives, including the pronephron, blood, myocardium, and vasculature, exhibited morphogenetic defects in the *sox32* mutant *casanova* (Alexander et al., 1999). Since the morphology of the IM was similarly aberrant in both the wild-type and *osr1* mutant contexts (G,H), it remains unclear whether *sox32* knockdown can rescue the production of IM in *osr1* mutants. Expression of *lhx1a* in the notochord (asterisk) was unaffected.

Scale bars: 100 μm.

SUPPLEMENTARY REFERENCES

Alexander, J., Rothenberg, M., Henry, G.L., Stainier, D.Y., 1999. *casanova* plays an early and essential role in endoderm formation in zebrafish. *Dev Biol* 215, 343-357.

Chestnut, B., Casie Chetty, S., Koenig, A.L., Sumanas, S., 2020. Single-cell transcriptomic analysis identifies the conversion of zebrafish Etv2-deficient vascular progenitors into skeletal muscle. *Nat Commun* 11, 2796.

Kohli, V., Schumacher, J.A., Desai, S.P., Rehn, K., Sumanas, S., 2013. Arterial and venous progenitors of the major axial vessels originate at distinct locations. *Dev Cell* 25, 196-206.

Mudumana, S.P., Hentschel, D., Liu, Y., Vasilyev, A., Drummond, I.A., 2008. *odd skipped related1* reveals a novel role for endoderm in regulating kidney versus vascular cell fate. *Development* 135, 3355-3367.

Perens, E.A., Garavito-Aguilar, Z.V., Guio-Vega, G.P., Pena, K.T., Schindler, Y.L., Yelon, D., 2016. Hand2 inhibits kidney specification while promoting vein formation within the posterior mesoderm. *eLife* 5:e19941.

Reischauer, S., Stone, O.A., Villasenor, A., Chi, N., Jin, S.W., Martin, M., Lee, M.T., Fukuda, N., Marass, M., Witty, A., Fiddes, I., Kuo, T., Chung, W.S., Salek, S., Lerrigo, R., Alsio, J., Luo, S., Tworus, D., Augustine, S.M., Mucenieks, S., Nystedt, B., Giraldez, A.J., Schroth, G.P., Andersson, O., Stainier, D.Y., 2016. Cloche is a bHLH-PAS transcription factor that drives haemato-vascular specification. *Nature* 535, 294-298.

Tomar, R., Mudumana, S.P., Pathak, N., Hukriede, N.A., Drummond, I.A., 2014. *osr1* Is Required for Podocyte Development Downstream of *wt1a*. *J Am Soc Nephrol* 25, 2539-2545.